Molecular Physics, Vol. 103, No. 19, 10 October 2005, 2621–2631

Taylor & Francis
Taylor & Francis Group

Correlation of dielectric properties, Raman spectra and calorimetric measurements of β-cyclodextrin-polyiodide complexes (β-cyclodextrin)$_2\cdot BaI_7\cdot 11H_2O$ and (β-cyclodextrin)$_2\cdot CdI_7\cdot 15H_2O$

V. G. CHARALAMPOPOULOS and J. C. PAPAIOANNOU*

Department of Chemistry, Laboratory of Physical Chemistry, National and Kapodistrian University of Athens, PO Box 64004, 157 10 Zografou, Athens, Greece

(*Received 6 December 2004; accepted 30 May 2005*)

The frequency and temperature dependence of real and imaginary parts of the dielectric constant ($\varepsilon', \varepsilon''$), the phase shift ($\varphi$) and the ac-conductivity (σ) of polycrystalline complexes (β-CD)$_2$·BaI$_7$·11H$_2$O and (β-CD)$_2$·CdI$_7$·15H$_2$O (β-CD = β-cyclodextrin) has been investigated over the frequency and temperature ranges 0–100 kHz and 140–420 K in combination with their Raman spectra, DSC traces and XRD patterns. The ε'(T), ε''(T) and φ(T) values at frequency 300 Hz in the range $T < 330$ K show two sigmoids, two bell-shaped curves and two minima respectively revealing the existence of two kinds of water molecule, the tightly bound and the easily movable. Both complexes show the transition of normal hydrogen bonds to flip-flop type at 201 K. In the β-Ba complex most of the eleven water molecules remain tightly bound and only a small number of them are easily movable. On the contrary, in the β-Cd case the tightly bound water molecules are transformed gradually to easily movable. Their DSC traces show endothermic peaks with onset temperatures 118°C, 128°C for β-Ba and 106°C, 123°C, 131°C for β-Cd. The peaks 118°C, 106°C, 123°C are related to the easily movable and the tightly bound water molecules, while the peaks at 128°C, 131°C are caused by the sublimation of iodine. The activation energy of Ba^{2+} ions is 0.52 eV when all the water molecules exist in the sample and 0.99 eV when the easily movable water molecules have been removed. In the case of β-Cd the corresponding activation energies are 0.57 eV and 0.33 eV. The Raman peaks at 179 cm^{-1}, 170 cm^{-1} and 165–166 cm^{-1} are due to the charge transfer interactions in the polyiodide chains.

1. Introduction

It is well known that α- and β-cyclodextrins (α-CD, β-CD) can form channel-type complexes when metal iodides (M^+I^-) are added to their aqueous solutions [1]. They display dimeric units in a head-to-head arrangement including polyiodide chains in their tubular cavities. The α-CD complexes are crystallized in four different crystal structures depending on the nature of metal (M) and their polyiodide chain consists of linear repeating units $I_3^- \cdot I_2$ or I_5^-. On the contrary, the β-CD complexes are crystallized in only one crystal form (monoclinic $P2_1$) for a variety of metal ions. According to the crystal structure of (β-CD)$_2$·KI$_7$·9H$_2$O [2] the polyiodide chain consists of discrete non-interacting I_7^- units. Each I_7^- unit has Z-like structure formulated as $I_2 \cdot I_3^- \cdot I_2$ in which the two I_2 units are included within the cavities of β-CD dimer and are nearly perpendicular to the I_3^- unit which is located between the β-CD dimers (figure 1 based on figure 4 of [2]). The structures of β-CD with other metals are isomorphous to that of (β-CD)$_2$·KI$_7$·9H$_2$O [2].

Since the electrical properties of polyiodide materials are of great interest [3], we have investigated the dielectric properties of α-CD complexes with Li, Cd, Ba and K metals [4, 5] and that of β-CD with Li and K metals [6].

All systems showed:

(a) the order–disorder transition that according to Saenger *et al.* [7, 8] is caused by the transformation of the normal hydrogen bonds to flip-flop type during the heating process. The transition temperature was indicated by a peak in the imaginary part

*Corresponding author. Email: jpapaio@cc.uoa.gr

Molecular Physics
ISSN 0026–8976 print/ISSN 1362–3028 online
http://www.tandf.co.uk/journals
DOI: 10.1080/00268970500195475

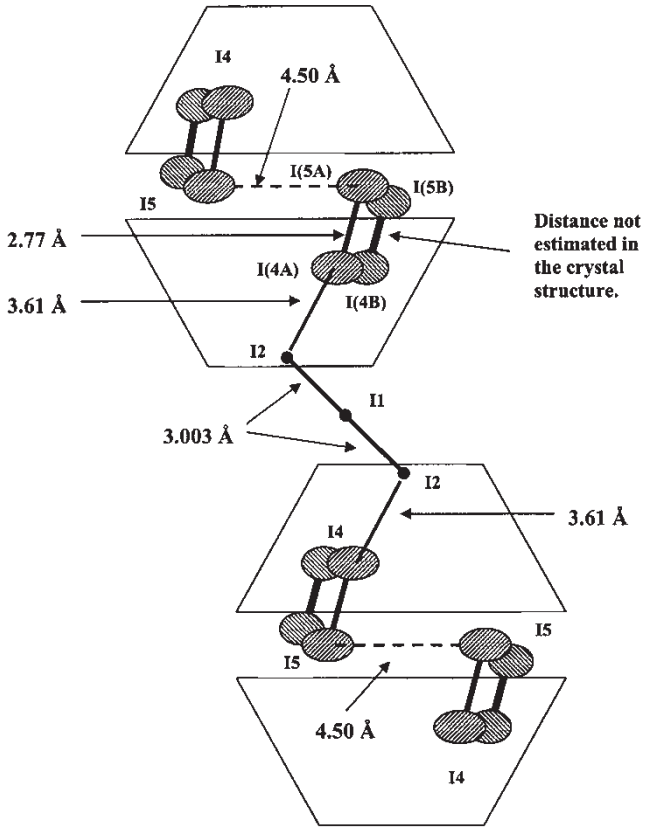

Figure 1. Geometry of polyiodide chain in the $(\beta\text{-CD})_2\cdot KI_7\cdot 9H_2O$ complex according to figure 4 of [2].

of the dielectric constant ε'' and by a minimum in the phase shift φ.

(b) ionic conductivity at temperatures higher than room temperature which decreases in the order:

$$\alpha\text{-}Ba^{2+} > \alpha\text{-}Li^{+} > \alpha\text{-}K^{+} > \alpha\text{-}Cd^{+}$$
$$\text{and } \beta\text{-}Li^{+} > \beta\text{-}K^{+}$$

(c) all systems except α-Li show two kinds of water molecules (tightly bound and easily movable). This was indicated in the temperature dependence ($T < 300$ K) of ε', ε'' and phase shift φ by two steps, two peaks and two minima respectively.

In the present work we investigate the dielectric properties of two more β-cyclodextrin–polyiodide inclusion complexes $(\beta\text{-cyclodextrin})_2\cdot BaI_7\cdot 11H_2O$ and $(\beta\text{-cyclodextrin})_2\cdot CdI_7\cdot 15H_2O$ named β-Ba and β-Cd respectively, over the frequency range 0–100 kHz and temperature range 140–420 K. Besides this, the Raman spectra in combination with calorimetric measurements are investigated in the temperature region 300–420 K.

2. Experimental

β-cyclodextrin, iodine, barium iodide and cadmium iodide were purchased from Fluka Chemica. The preparation of both samples was carried out according to [1]. One gram of β-CD was dissolved in 80 ml of distilled water at room temperature under stirring until the solution became almost saturated. Then 0.46 g barium iodide and 0.44 g solid iodine were added simultaneously to the solution and it was heated to 70°C for 20–25 minutes. The hot solution was transferred quickly through a folded filter to an empty cylindric glassy flask (100 ml) which was covered with Teflon and then immersed in a Dewar flask (500 ml) containing hot water (~70°C). After two days, very fine reddish-brown thin needles of β-Ba were grown with uniform composition, held back in a Buchner filter and dried in air. For β-Cd we used 1 gram β-CD, 0.42 g cadmium iodide and 0.44 g solid iodide and very fine reddish-brown thin needles of β-Cd were grown with uniform composition, in a similar way to the β-Ba case. The water content of the crystals was determined by the use of thermogravimetric analysis (NETZSCH-STA 409 EP, Controller TASC 414/3, heating rate $5°C\,min^{-1}$). The β-Ba and β-Cd complexes were found to contain eleven and fifteen water molecules, respectively (figure 2(*a*), (*b*)). So, the general compositions are $(\beta\text{-CD})_2\cdot BaI_7\cdot 11H_2O$ and $(\beta\text{-CD})_2\cdot CdI_7\cdot 15H_2O$.

Pressed pellets of powdered samples, 20 mm in diameter with thickness 1.05 mm for β-Ba and 0.96 mm for β-Cd, were prepared with a pressure pump (Riken Power model P-1B) at room temperature. Two platinum foil electrodes were pressed at the same time with the sample. The pellet was then loaded in a temperature-controlled chamber, between two brass rods accompanied by a compression spring. A K-type thermocouple was kept close to the sample, and the whole cell was kept under N_2 atmosphere.

The dielectric measurements were taken using a low-frequency (0–100 kHz) dynamic signal analyser (DSA-Hewlett-Packard 3561A), at the temperature range of 140–420 K, operating at both frequency and time domains which is capable of measuring amplitude and phase accurately relative to a trigger signal. The instrument can measure simultaneously the amplitude of the impedance vector and the phase shift of the sample under consideration at each frequency value in the region between 0 Hz and 100 kHz. DSA applies a signal of periodic noise $72.5\,mV_{rms}$ to the sample connected in series with a fixed known resistance $R_i = 9.85\,k\Omega$ for $T < 300$ K and $R_I = 0.975\,k\Omega$ for $T > 300$ K. The voltage drop across the external resistance V_i was kept at less than 10% of the applied, to minimize the effects of R_i on the phase difference.

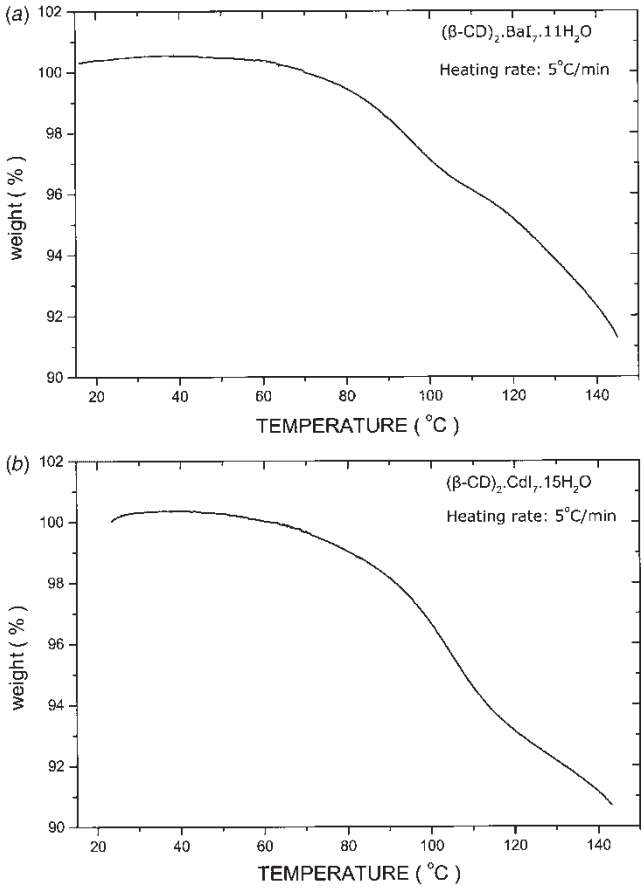

Figure 2. Thermogravimetric analysis (TGA) of (*a*) $(\beta\text{-CD})_2\cdot BaI_7\cdot 11H_2O$; (*b*) $(\beta\text{-CD})_2\cdot CdI_7\cdot 15H_2O$.

Initially the sample was short-circuited and the amplitude spectrum (signal level as a function of frequency) and the phase spectrum (phase as a function of frequency) of the periodic noise signal across the resistance were displayed simultaneously and stored in memories M_1, M_2 of DSA. Thereafter, the sample was connected and the same procedure was repeated. The new amplitude and phase spectra of signal across the resistance R_i were displayed also and stored in the buffer memory of DSA. Then by use of the 'math function' the amplitude voltage ratio V_i/V versus frequency and the phase shift (φ) versus frequency of the corresponding traces were calculated. This data was stored in the internal non-volatile memory, where up to 40 contiguous time records could be stored for additional processing. The above data acquisition time was of the order 4 ms for a full impedance spectrum. The data can be transferred to a PC through a HP 82335 Interface Bus (IEEE-488), where it can be stored and analysed by a software program. The imaginary and real parts of either impedance or dielectric constant versus frequency and temperature and the Cole–Cole plots can be calculated and plotted [9].

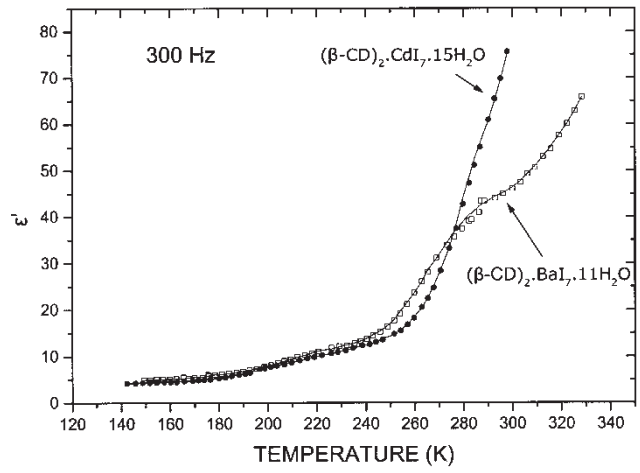

Figure 3. Temperature dependence of real (ε') part of the dielectric constant of $(\beta\text{-CD})_2\cdot BaI_7\cdot 11H_2O$ and $(\beta\text{-CD})_2\cdot CdI_7\cdot 15H_2O$ at 300 Hz.

The differential scanning calorimetry (DSC) method (Perkin Elmer DSC-4 instrument) was used with a thermal analysis data station (TADS) system for all calorimetric measurements.

The Raman spectra were obtained at $4\,cm^{-1}$ resolution from $3500\,cm^{-1}$ to $100\,cm^{-1}$ with interval $1\,cm^{-1}$ using a Perkin-Elmer NIR FT-spectrometer (Spectrum GX II) equipped with CCD detector. The measurements were performed at a temperature range of 30–120°C (303–393 K). The laser power and spot (aNd:YAG at 1064 nm) were controlled to be constant at 50 mW during the experiments. 500 scans were accumulated and backscattering light was collected.

X-ray powder diffraction patterns were obtained with a Siemens D 5000 diffractometer (CuKα1 = 1.5406 Å, CuKα2 = 1.5444 Å, scan range: 5–55° 2θ, monochromator: graphite crystal, scan speed: $0.045\,2\theta\cdot s^{-1}$). The calculation of the X-ray powder diffraction pattern was performed by the computer program *Powder Cell 2.3* developed by G. Nolze and W. Kraus [10], using the single crystal $(\beta\text{-CD})_2\cdot KI_7\cdot 9H_2O$ diffraction data reported by Saenger in [2].

3. Results

3.1. *Temperature dependence of ε′, ε″ and phase shift*

The temperature dependence of ε' and ε'' over the range 140–330 K at frequency 300 Hz is shown in figures 3 and 4(*a*, *b*) for both complexes $(\beta\text{-CD})_2\cdot BaI_7\cdot 11H_2O$ and $(\beta\text{-CD})_2\cdot CdI_7\cdot 15H_2O$.

In the $(\beta\text{-CD})_2\cdot BaI_7\cdot 11H_2O$ complex ε' increases in a double-sigmoid fashion from 4.9 at low temperatures $T = 150$ K, to 12.4 at 232 K and then to 46.1 at temperature 300 K. The inflection point of the first

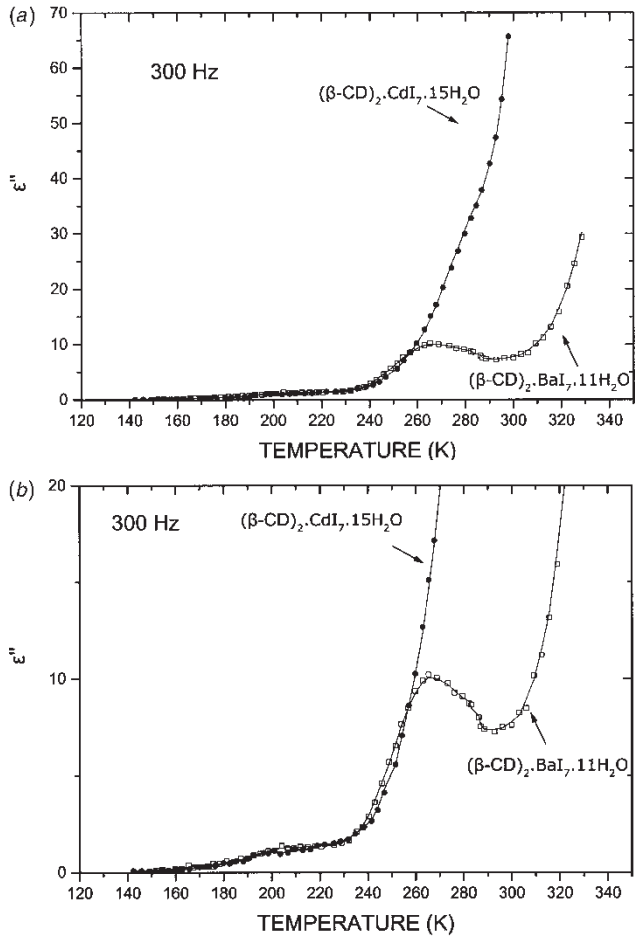

Figure 4. (*a*) Temperature dependence of imaginary (ε'') parts of the dielectric constant of (β-CD)$_2$·BaI$_7$·11H$_2$O and (β-CD)$_2$·CdI$_7$·15H$_2$O at 300 Hz; (*b*) ε'' versus T showing clearly the first bell-shaped curve of (β-CD)$_2$·BaI$_7$·11H$_2$O and (β-CD)$_2$·CdI$_7$·15H$_2$O.

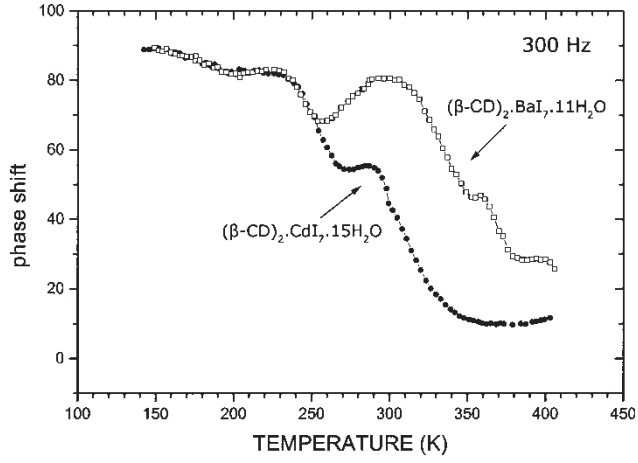

Figure 5. Temperature dependence of phase shift of (β-CD)$_2$·BaI$_7$·11H$_2$O and (β-CD)$_2$·CdI$_7$·15H$_2$O at 300 Hz.

sigmoid is observed at 201.2 K ($\varepsilon' = 8.1$) and that of the second sigmoid at 276.1 K ($\varepsilon' = 35.7$). Above 300 K, ε' continues to increase, so that $\varepsilon' = 65.8$ at 328 K. The variation in dielectric loss ε'' with temperature gives a double bell-shaped curve with first peak value $\varepsilon'' = 1.4$ at 204.1 K and second peak value $\varepsilon'' = 10.2$ at 265.2 K. For $T > 300$ K, ε'' increases more rapidly so that at 328 K $\varepsilon'' = 29.4$. By increasing the frequency of the applied field to 1 kHz, the two sigmoid curves in the ε' versus T plot and the double bell-shaped curve in the ε'' versus T plot remain distinguished. The same situation is observed for higher applied frequencies (10–100 kHz).

In the (β-CD)$_2$·CdI$_7$·15H$_2$O complex the temperature dependence of ε' is similar to the (β-CD)$_2$·BaI$_7$·11H$_2$O complex but the temperature dependence of ε'' is not similar. The ε' increases in a double-sigmoid fashion from 4.2 at low temperatures $T < 150$ K to 12.3 at 238.5 K and then to 60.8 at temperature 290 K. The inflection point of the first sigmoid is observed at 201 K ($\varepsilon' = 7.7$) and that of the second sigmoid at 284.4 K ($\varepsilon' = 51.0$). An interesting observation is that above 250 K, ε' increases rapidly so that at temperature 300 K, $\varepsilon' = 75.6$ and the second sigmoid is hardly distinguished. The ε'' versus T plot shows, a single bell-shaped curve with peak value 1.1 at 201 K and a shoulder with value 23.8 at 274.1 K. Above 250 K, ε'' increases fast with temperature so that at 300 K, $\varepsilon'' = 65.6$. By increasing the frequency of the applied field to 1 kHz, the double sigmoid of the ε' versus T plot and the bell-shaped curve and the shoulder of ε'' versus T plot, remain distinguished. The same qualitative picture is observed for the other, higher fixed frequencies in the range 10–100 kHz.

The phase shift φ of (β-CD)$_2$ · BaI$_7$ · 11H$_2$O at a fixed frequency of 300 Hz (figure 5) over the range 140–400 K, presents two topical minimum values in the temperature region $T < 330$ K and two topical minimum values (like plateau regions) at $T > 330$ K. Specifically it drops from 89.4° at 150 K to a minimum value of 82° at 201 K, then it increases to 83.1° at 226 K and decreases rapidly to the minimum value 68.2° at 257 K, it increases again to 80.5° at 296 K then drops rapidly to the plateau value 46.2° at 355–358 K and finally drops rapidly to the other plateau value 28.5° at 385–394 K. At higher fixed frequencies the two topical minimum and plateau regions are still distinguished but slightly shifted to higher temperatures. Similarly, the phase shift φ of (β-CD)$_2$·CdI$_7$·15H$_2$O at a fixed frequency of 300 Hz, presents two topical minimum values at $T < 330$ K and one extended minimum at $T > 330$ K. It drops from 88.8° at 142 K to a minimum value of 81.7° at 201 K, then it increases to 82.9° at 216 K and it decreases rapidly to 54.3° at 274 K; then it increases to 55.4° at 284 K and finally it decreases rapidly to the minimum value 9.7° at 379 K. For higher fixed frequencies, the two

topical minimum values are hardly distinguished and shifted to lower temperatures.

3.2. *Temperature dependence of conductivity*

The variation with temperature of ac conductivity ($\ln \sigma$ versus $1/T$) of the β-Ba complex at 300 Hz is shown in figure 6 during the heating process. This plot shows the sigmoid curves (a) and (b) in the temperature ranges $4.30\,K^{-1} < 10^3/T$ and $3.41\,K^{-1} < 10^3/T < 4.30\,K^{-1}$ respectively, and the linear parts (c), (d), in the temperature range $2.49\,K^{-1} < 10^3/T < 3.41\,K^{-1}$. Finally at temperatures higher than 128°C ($10^3/T < 2.49\,K^{-1}$) there is an abrupt increase of ac-conductivity, part (e), as a consequence of iodine's sublimation. Similar results are found for the β-Cd complex. It presents two sigmoid curves in the temperature ranges $4.32\,K^{-1} < 10^3/T$ and $3.3\,K^{-1} < 10^3/T < 4.32\,K^{-1}$ and the linear parts (c) and (d) in the temperature range $2.48\,K^{-1} < 10^3/T < 3.3\,K^{-1}$. In the same way at temperatures higher than 130°C an abrupt increase of σ is observed. The conductivity values of β-Ba and β-Cd samples are almost the same over the temperature range 150–260 K ($3.8\,K^{-1} < 10^3/T < 6.6\,K^{-1}$) but at higher temperatures the β-Cd values are considerably higher than those of β-Ba. Thermal hysteresis was observed for the β-Ba sample (figure 7), but totally absent for the β-Cd sample (figure 8).

3.3. *Calorimetric measurements*

The DSC trace of $(\beta\text{-CD})_2{\cdot}CdI_7{\cdot}15H_2O$ (figure 9) with scan rate $10\,min^{-1}$, shows three endothermic peaks with onset temperatures 106°C, 123°C and 131°C, over a temperature range of 50°C. In the DSC trace of

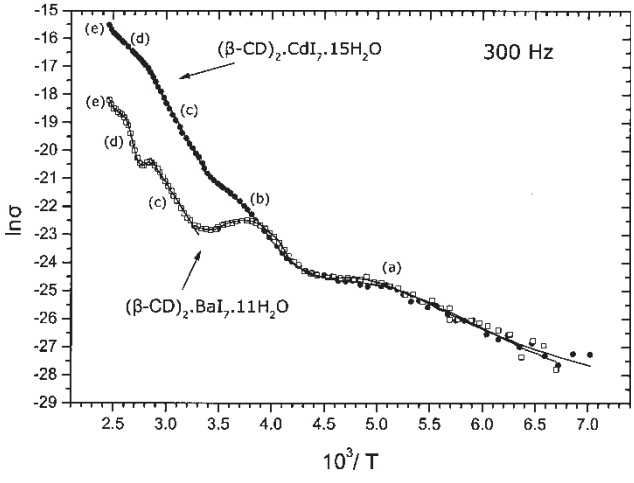

Figure 7. Temperature dependence of ac-conductivity ($\ln \sigma$ versus $1/T$) for the complex $(\beta\text{-CD})_2{\cdot}BaI_7{\cdot}11H_2O$ during the cooling and heating process, at frequency 300 Hz.

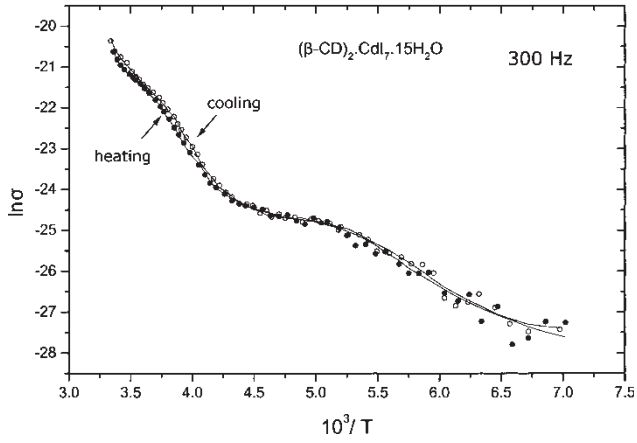

Figure 8. Temperature dependence of ac-conductivity ($\ln \sigma$ versus $1/T$) for the complex $(\beta\text{-CD})_2{\cdot}CdI_7{\cdot}15H_2O$ during the cooling and heating process, at frequency 300 Hz.

Figure 6. Temperature dependence of ac-conductivity ($\ln \sigma$ versus $1/T$) for the complexes $(\beta\text{-CD})_2{\cdot}BaI_7{\cdot}11H_2O$ and $(\beta\text{-CD})_2{\cdot}CdI_7{\cdot}15H_2O$ at 300 Hz.

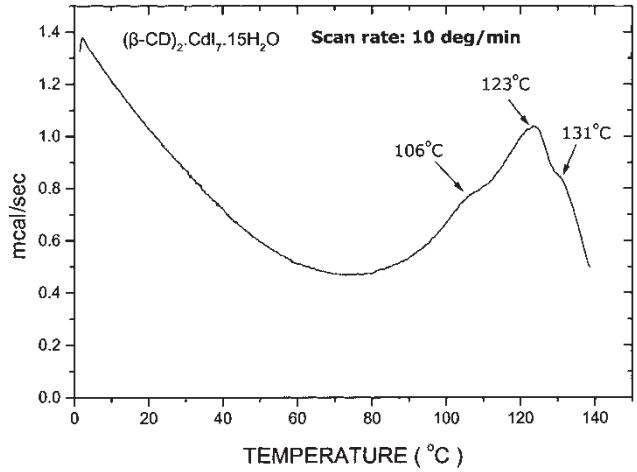

Figure 9. DSC thermogram of $(\beta\text{-CD})_2{\cdot}CdI_7{\cdot}15H_2O$: heating rate 10°C/min.

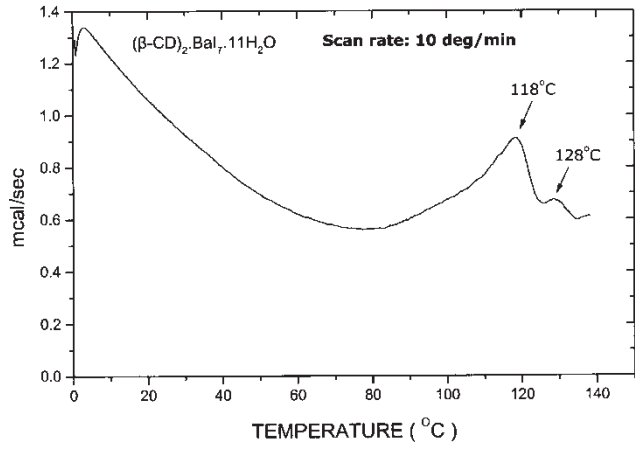

Figure 10. DSC thermogram of $(\beta\text{-CD})_2{\cdot}BaI_7{\cdot}11H_2O$: heating rate 10°C/min.

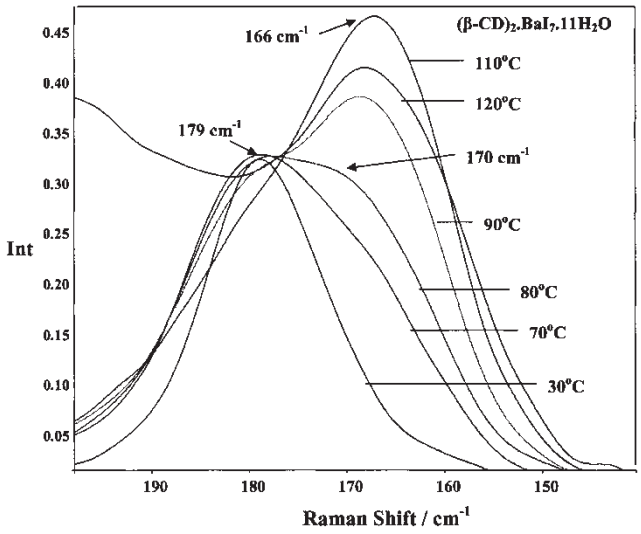

Figure 11. Raman spectra of $(\beta\text{-CD})_2{\cdot}BaI_7{\cdot}11H_2O$ complex at 30–120°C.

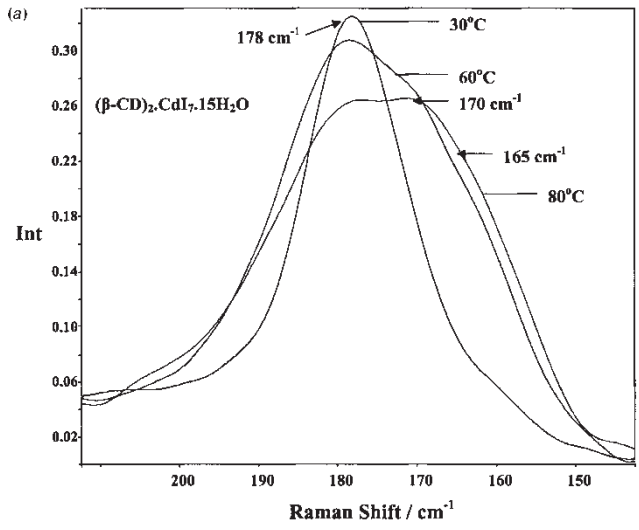

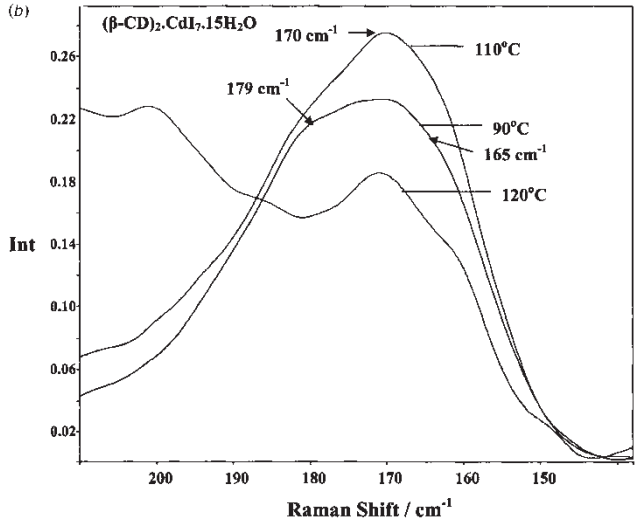

Figure 12. (*a*) Raman spectra of $(\beta\text{-CD})_2{\cdot}CdI_7{\cdot}15H_2O$ complex at 30–80°C; (*b*) Raman spectra of $(\beta\text{-CD})_2{\cdot}CdI_7{\cdot}15H_2O$ complex at 90–120°C.

$(\beta\text{-CD})_2{\cdot}BaI_7{\cdot}11H_2O$ (figure 10) two endothermic peaks are observed with onset temperatures 118°C and 128°C, over a temperature range of 42°C.

3.4. *Raman spectra*

The Raman spectra of β-Ba complex in figure 11 for different temperatures 30°C, 70°C, 80°C, 90°C, 110°C, 120°C, displays a strong peak at 179 cm^{-1} at 30°C with almost constant intensity as the temperature increases. At 70°C a shoulder arises at 170 cm^{-1} with peak value 0.20 and intensity increasing with temperature, which is shifted to the value 166 cm^{-1} in the temperature range 90–120°C. The peak intensity takes a maximum value at 110°C (0.46) and then decreases to 0.40 at 120°C.

Figure 12 shows the Raman spectra of β-Cd complex for the different temperatures 30°C, 60°C, 80°C, 90°C, 110°C, 120°C. It displays a strong peak at 178 cm^{-1} for temperature 30°C with decreasing intensity by temperature, in the range 30–80°C. For temperature 80°C a broad double peak is observed at 178 cm^{-1} and 170 cm^{-1} with peak values 0.26 and 0.25 respectively, and a small shoulder arises at 165 cm^{-1}. At 90°C three peaks can be distinguished at 179 cm^{-1}, 170 cm^{-1} and 165 cm^{-1}, whose intensities take a maximum value at 110°C. Finally at 120°C the 170 cm^{-1} peak and the 165 cm^{-1} shoulder still remain.

3.5. *X-ray powder diffraction*

Figure 13 shows experimental X-ray powder diffraction patterns of $(\beta\text{-CD})_2{\cdot}BaI_7{\cdot}11H_2O$, $(\beta\text{-CD})_2{\cdot}CdI_7{\cdot}15H_2O$ complexes and the simulated pattern calculated

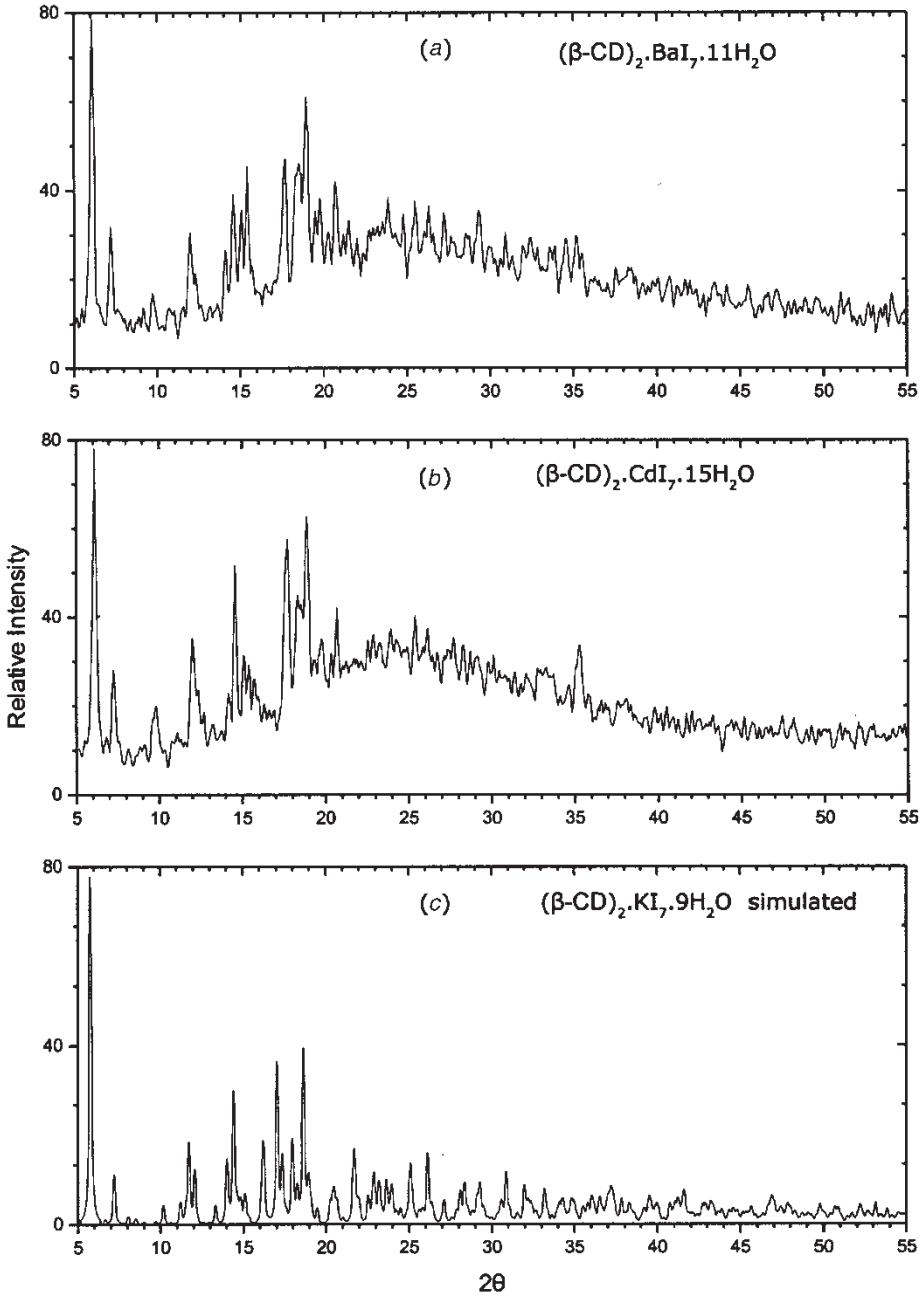

Figure 13. Experimental X-ray powder diffraction patterns of (*a*) (β-CD)$_2$·BaI$_7$·11H$_2$O and (*b*) (β-CD)$_2$·CdI$_7$·15H$_2$O complexes and (*c*) calculated X-ray powder diffraction pattern from single crystal data of (β-CD)$_2$·KI$_7$·9H$_2$O complex.

from the single-crystal X-ray diffraction data of the (β-CD)$_2$·KI$_7$·9H$_2$O complex [2]. It is obvious that β-Ba, β-Cd complexes exhibit similar XRD patterns (Bragg reflections at the same 2θ angles) which are in good agreement with the calculated of β-K complex. Therefore the three complexes are isomorphous as it was foretold by Saenger [2]. The hump at around 25° in (*a*), (*b*) is caused by the presence of some poorly crystalline material, while the multitude of peaks at higher 2θ angles is not a result of phase impurities but corresponds to weak Bragg reflections as is depicted in the calculated pattern (*c*). We also note that some diffraction peaks exhibit larger relative intensities than those of the simulated pattern owing to the non-random distribution of crystal orientations (preferred orientation effects). Because of the observed hump in the experimental patterns, it is difficult to depict their realistic differences with the theoretical one.

4. Discussion

The dielectric behaviour of both complexes β-Ba and β-Cd is similar to that of β-Li and β-K published in [6]. That is, the temperature dependence of ε', ε'' and φ in the range $T < 330\,\mathrm{K}$ shows two sigmoids, two bell-shaped curves and two minima respectively. This behaviour reveals the existence of two kinds of water molecules in both complexes, tightly bound and the easily movable water molecules.

The fact that the first sigmoid of $\varepsilon'(T)$ at low temperatures or the first peak of $\varepsilon''(T)$ or the first minimum of $\varphi(T)$ is the same for both β-Ba and β-Cd complexes is caused by the same number of normal hydrogen bonds transformed to flip-flop type according to Saenger [7, 8]:

$$H_B{-}O\cdots H_A{-}O \Leftrightarrow O{-}H_B\cdots O{-}H_A. \qquad (1)$$

The order–disorder transition temperature is found at 201 K for both complexes in figure 5.

The second $\varepsilon'(T)$ sigmoid of β-Cd is hardly distinguished because of the protonic conductivity and the transformation of some tightly bound water molecules to easily movable by the increased temperature. However, in the case of β-Ba the second sigmoid is clearly distinguished and the second loss peak of $\varepsilon''(T)$ is also clear. That means that as the temperature increases most of the eleven water molecules per dimer remain tightly bound and only a small number of them are easily movable. For this reason the DSC trace of β-Ba shows the slab peak at 118°C, which corresponds to the tightly bound water molecules. On the contrary, in β-Cd the number of easily movable water molecules continuously increases as the temperature increases according to the transformation (2):

$$(H_2O)_{\mathrm{tightlybound}} \Leftrightarrow (H_2O)_{\mathrm{easilymovable}}, \qquad (2)$$

resulting in a progressive rise of $\varepsilon'(T)$ and $\varepsilon''(T)$ values, altering their shape. For this reason the DSC trace of β-Cd shows a first peak at 106°C, which corresponds to the easily movable water molecules and a second peak at 123°C due to the tightly bound water molecules. The third peak of β-Cd (figure 9) at 131°C and the second peak of β-Ba (figure 10) at 128°C, are caused by the sublimation of iodine.

The above discussion is referred to the temperature region $T < 330\,\mathrm{K}$, where all the water molecules exist in the crystal lattice. At higher temperatures $T > 330\,\mathrm{K}$, additional effects are appeared in the electrical properties of both β-Ba and β-Cd complexes related to the ionic conductivity of metal ions, the removal of water molecules and the contribution of polyiodide chain. All these effects are depicted in the φ versus T and $\ln\sigma$ versus $1/T$ plots, in figures 5 and 6, respectively. The dielectric parameters ε', ε'' are no longer sensitive to these effects, because of the large protonic and ionic conductivity of metal cations. The phase shift of β-Ba for $T > 300\,\mathrm{K}$ shows two transformations (minimum degenerated in plateau), that happen in the temperature ranges (355–358 K) and (385–405 K) which are related to the removal of the easily movable water molecules and tightly bound water molecules respectively. In the case of β-Cd the broad minimum at 379 K shows the progressive transformation of tightly bound water molecules to easily movable ones and the removal from the crystal lattice, as was discussed earlier in the DSC traces.

The different components contributing to the conductivity are detected from the $\ln\sigma$ versus $1/T$ plot of β-Ba (figure 6), indicated by the sigmoids (a), (b) and the linear parts (c), (d) and (e). The low temperature sigmoid (a), for $T < 232.5\,\mathrm{K}$ ($10^3/T > 4.30\,\mathrm{K}^{-1}$), is due to the H^+ and OH^- of the normal hydrogen bonds of the water and the β-CD molecules, whereas the high temperature sigmoid (b) for $232.5\,\mathrm{K} < T < 293.5\,\mathrm{K}$ ($3.41\,\mathrm{K}^{-1} < 10^3/T < 4.30\,\mathrm{K}^{-1}$) is caused by the transformation of some normal hydrogen bonds to flip-flop type, a process which creates disordered atoms. The linear part (c) over the range $307\,\mathrm{K} < T < 345\,\mathrm{K}$ ($2.90\,\mathrm{K}^{-1} < 10^3/T < 3.25\,\mathrm{K}^{-1}$), with activation energy $E_\alpha = 0.52\,\mathrm{eV}$ as calculated from the Arrhenius equation $\sigma = \sigma_0 \exp(-E_w/2K_BT)$, is due to the contribution of metallic cations Ba^{2+} which move under the applied alternate field. Since β-Ba complex has isomorphous crystal structure with that of β-K, we consider that the metal cation Ba^{2+} is fourfold coordinated to two water molecules and two O(6) hydroxyl groups in a tetrahedral arrangement in a similar way to that of K^+ [2]. Initially the above coordination shell restricts the movement of Ba^{2+} ions, rendering them unable to have an essential contribution to the ac-conductivity. By increasing the temperature the tetrahedral arrangement is being perturbed resulting in the release of positive ions, which are free to oscillate back and forth with the frequency of the field and to contribute to the total ac-conductivity. During this process there is a gradual transformation of the tightly bound water molecules to easily movable ones, which increases the protonic conductivity in the water-net, via the Grotthus mechanism [11, 12].

At temperatures higher than 70–80°C ($10^3/T < 2.9\,\mathrm{K}^{-1}$) the increasing rate of conductivity is reduced since the easily movable water molecules start to escape, as depicted in the DSC trace of figure 10. Next, as the

temperature increases the rest of the tightly bound water molecules become gradually easily movable resulting in the rapid increase of conductivity (linear part (d)) with higher activation energy $E_\alpha = 0.99$ eV, calculated as above. At temperatures higher than 112°C ($10^3/T < 2.6\,K^{-1}$) the conductivity rate is decreasing again because of the continuous removal process of the water molecules. According to the DSC trace of figure 10, the total number of water molecules have been removed at 125°C. Finally at temperatures higher than 128°C ($10^3/T < 2.49\,K^{-1}$) the abrupt increase of ac-conductivity (linear part (e)) is due to the sublimation of iodine molecules (peak at 128°C in figure 10), which shorts the I_7^- units and permits the charge transfer interaction between them [13]. The duration of this effect lasts few minutes and in the end the conductivity takes very low values. So it is clear that the contribution of I_7^- units in the conductivity at temperatures lower than 128°C, is negligible and the I_7^- charge is localized.

Considering the $I\cdots I$ distances of I_7^- units of β-Ba similar to that of β-K additional information is found from the temperature dependence of Raman spectra (figure 11). In the temperature range 30–70°C where all the water molecules exist in the lattice, the Raman spectra exhibit the peak at 179 cm^{-1} with the same almost intensity. In the temperature range 70–80°C, a second peak at 170 cm^{-1} coexists with the initial peak at 179 cm^{-1} and finally at temperatures higher than 90°C the Raman peak is shifted to the value 166 cm^{-1} with maximum intensity at 110°C where some water molecules still exist in the lattice (the water molecules are totally removed at 125°C). Almost the same Raman peaks 179 cm^{-1}, 170 cm^{-1} and 165 cm^{-1}, were found in the cases of isomorphous β-K, β-Li complexes [14] in the corresponding temperature ranges.

The above Raman peaks are due to the polyiodide chain $I_2\cdot I_3^-\cdot I_2$ and reflect the interactions between the I_3^- and the two I_2 units in each dimer [15]. The iodine atoms I1, I2 of the central I_3^- unit show full occupance (1,0) with I1–I2 separation 3.003 Å (figure 1). The atoms I4, I5 of I_2 units are disordered in positions with main occupancies I(4A) = 0.89 and I(5A) = 0.70 and positions with minor occupancies I(4B) = 0.15 and I(5B) = 0.14. In the case of main occupancies the separation distance of iodine atoms in I_2 units is I(4A)–I(5A) = 2.77 Å and the separation between I_2 and I_3^- units is I2–I(4A) = 3.61 Å. In the case of minor occupancies the corresponding positions display shorter distances (not estimated in the crystal structure) of β-K.

A linear correlation of FT-Raman frequencies ν(I–I) versus the d(I–I) bond distances has been obtained for different weak complexes with I_2 [16]. As the interiodine distance increases, the FT-Raman band moves to lower frequency with respect to the value 180 cm^{-1} reported for solid iodine [17]. The Raman peaks at 179 cm^{-1}, 170 cm^{-1} and 166 cm^{-1} found experimentally in figure 11 correspond to d(I–I) distances 2.72 Å, 2.75 Å and 2.77 Å respectively. According to this, the strong band at 166 cm^{-1} could be assigned to the two disordered atoms of I_2 units I(4A), I(5A) with the longer distances I(4A)–I(5A) = 2.77 Å, while the initial band at 179 cm^{-1} to an average d(I–I) distance 2.72 Å, resultant of the simultaneous main and minor occupancies of iodine atoms I(4A), I(5A) and I(4B), I(5B) in the dimers. This correspondence indicates that the disordered atoms I(4B), I(5B) with minor occupancies are transformed to I(4A), I(5A) with main occupancies as the temperature increases (order–disorder transition, figure 14). The peak at 170 cm^{-1} corresponding to d(I–I) = 2.75 Å is attributed to an intermediate state in which a charge transfer interaction $I_2\cdots I_3^-$ takes place due to the symmetric stretch of iodine molecules [18]. So during the heating process, a lengthening of I(4B)–I(5B) distances of I_2 units to 2.77 Å takes place. The Raman peak corresponding to interiodine distance I(1)–I(2) = 3.003 Å of the I_3^- units, according to the above ν(I–I) versus d(I–I) correlation is located at frequencies smaller than that of 100 cm^{-1} which was not possible to detect in this low frequency region. The displacement of I(4B), I(5B)

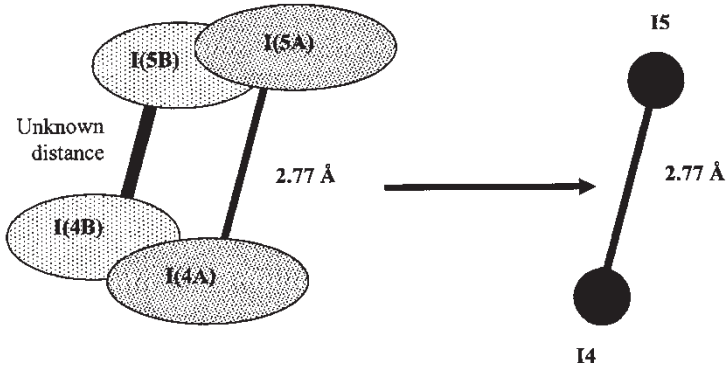

Figure 14. Order–disorder transition of I_2 molecules in I_7^- ions.

atoms of I_2 units as a result of a charge transfer interaction $I_2 \cdots I_3^-$ changes the distribution of electronic density, which remains localized since there is no interaction between the subsequent I_7^- units (I(5)–I(5) = 4.50 Å) [2] and has very little contribution to the conductivity.

Similar behaviour is observed for the β-Cd complex. The $\ln\sigma$ versus $1/T$ plot (figure 6), shows the two sigmoid curves (a) and (b) in the temperature ranges $T < 210\,\mathrm{K}$ $(10^3/T > 4.77\,\mathrm{K}^{-1})$ and $210\,\mathrm{K} < T < 303\,\mathrm{K}$ $(3.3\,\mathrm{K}^{-1} < 10^3/T < 4.8\,\mathrm{K}^{-1})$ respectively and the linear parts (c), (d) and (e) in the temperature ranges $303\,\mathrm{K} < T < 359\,\mathrm{K}$ $(2.8\,\mathrm{K}^{-1} < 10^3/T < 3.3\,\mathrm{K}^{-1})$, $T > 359\,\mathrm{K}$ $(10^3/T < 2.8\,\mathrm{K}^{-1})$ and $T > 400\,\mathrm{K}$ $(10^3/T < 2.5\,\mathrm{K}^{-1})$ respectively. The fact that in the low temperature region $T < 260\,\mathrm{K}$ the conductivity variation with temperature is the same for both β-Ba and β-Cd complexes, is caused by the same number of normal hydrogen bonds transformed to flip-flop type as was discussed earlier:

$$\sigma_{\beta-\mathrm{Cd}} = \sigma_{\beta-\mathrm{Ba}} \quad \text{for } T < 260\,\mathrm{K}.$$

The increasing upper plateau values by temperature in the case of (b) sigmoid of β-Cd shows that the number of tightly bound water molecules transformed to easily movable ones, increases continuously as temperature increases though in the β-Ba case only a small number of tightly bound water molecules are transformed according to the equation (2). These are in full agreement with the already discussed DSC traces. The linear part (c) is attributed to the contribution of metallic cations Cd^{2+} to the conductivity which is higher than that of β-Ba because the lighter cation Cd^{2+} is transported easier than the Ba^{2+} under the applied alternate field that is:

$$\sigma_{\beta\text{-Cd}} > \sigma_{\beta\text{-Ba}} \quad \text{for } T < 260\,\mathrm{K}.$$

The activation energies of the linear parts (c) and (d) are 0.57 eV and 0.33 eV respectively, calculated as before. The linear part (e) is directly related to the sublimation of iodine confirmed by the DSC trace of β-Cd (figure 9).

This aspect is in agreement with the results found for β-CD complexes with Li^+, K^+ [14]. In the Raman spectra of β-Cd the peaks at $179\,\mathrm{cm}^{-1}$, $170\,\mathrm{cm}^{-1}$ and $165\,\mathrm{cm}^{-1}$ are explained in the same way as was discussed for the β-Ba complex. The fact that the Raman peak at $170\,\mathrm{cm}^{-1}$ still remains at 120°C is due to the restrictions caused by the remaining tightly bound water molecules which disallow the lengthening of I(4B), I(5B) atoms.

Finally, we point out that the presence of non-crystalline material (XRD hump) does not affect the above discussion about the macroscopic dielectric properties, since the fundamental building blocks (β-CD dimers, coordinated metal ions and I_7^- units) are expected to be unchanged.

5. Conclusions

Both $(\beta\text{-CD})_2\cdot BaI_7\cdot 11H_2O$ and $(\beta\text{-CD})_2\cdot CdI_7\cdot 15H_2O$ complexes show two kinds of water molecules, the tightly bound and the easily movable water molecules, as was found in the cases of $(\beta\text{-CD})_2\cdot KI_7\cdot 8H_2O$ and $(\beta\text{-CD})_2\cdot LiI_7\cdot 8H_2O$ [6].

Both samples present the transformation of normal hydrogen bonds to flip-flop type at 201 K and the transformation of some tightly bound water molecules to easily movable water molecules according to the scheme:

$$(H_2O)_{\mathrm{tightlybound}} \Leftrightarrow (H_2O)_{\mathrm{easilymovable}}.$$

In the case of β-Ba complex most of the eleven water molecules per dimer remain tightly bound and only a small number of them are easily movable, though in the β-Cd case the number of easily movable water molecules increases continuously by increasing the temperature, resulting in a progressive rise of $\varepsilon'(T)$, $\varepsilon''(T)$ values. The endothermic peaks of their DSC traces with onset temperatures 118°C, for β-Ba and 106°C, 123°C for β-Cd are related to the easily movable and the tightly bound water molecules, while the peaks at 128°C, 131°C respectively are caused by the sublimation of iodine.

For $T < 260\,\mathrm{K}$, the ac-conductivity values are the same ($\sigma_{\beta\text{-Cd}} = \sigma_{\beta\text{-Ba}}$) while at $T > 260\,\mathrm{K}$ they are unequal ($\sigma_{\beta\text{-Cd}} > \sigma_{\beta\text{-Ba}}$). The different components contributing to the conductivity are detected from the $\ln\sigma$ versus $1/T$ plots of the two complexes, indicated by the sigmoids (a), (b) and the linear parts (c), (d) and (e). The low temperature sigmoids (a), for $T < 232.5\,\mathrm{K}$ are due to the H^+ and OH^- of the normal hydrogen bonds of the water and the β-CD molecules, whereas the high temperature sigmoids (b) for $232.5\,\mathrm{K} < T < 307\,\mathrm{K}$ are caused by the transformation of some normal hydrogen bonds to flip-flop type. The linear parts (c), (d) over the range $307\,\mathrm{K} < T < 400\,\mathrm{K}$ with activation energies 0.52 eV, 0.99 eV for β-Ba and 0.57 eV, 0.33 eV for β-Cd are related to the contribution of the metal ions and the removal of the water molecules to the ac-conductivity.

The Raman peaks at $179\,\mathrm{cm}^{-1}$, $170\,\mathrm{cm}^{-1}$ and 165–$166\,\mathrm{cm}^{-1}$ indicate charge transfer interactions in the I_7^- units and that their negative charge remains localized with negligible contribution to the conductivity until the sublimation of iodine starts.

Acknowledgements

This work was partly supported by Grant No. 70/4/3347SARG, NKUA. We thank Professor K. Viras for his assistance with the Raman spectra and DSC thermograms.

References.

[1] M. Noltmeyer, W. Saenger. *J. Am. chem. Soc.*, **102**, 2710 (1980).
[2] C. Betzel, B. Hingerty, M. Noltmeyer, G. Weber, W. Saenger. *J. incl. Phenom.*, **1**, 181 (1983).
[3] P. Svensson, L. Kloo. *Chem. Rev.*, **103**, 1649 (2002).
[4] T. Ghikas, J. Papaioannou. *Mol. Phys.*, **100**, 673 (2001).
[5] J. Papaioannou, T. Ghikas. *Mol. Phys.*, **101**, 2601 (2003).
[6] J. Papaioannou. *Mol. Phys.*, **102**, 95 (2004).
[7] C. Betzel, W. Saenger, B.E. Hingerty, G.M. Brown. *J. Am. chem. Soc.*, **106**, 7545 (1984).
[8] V. Zabel, W. Saenger, S.A. Mason. *J. Am. chem. Soc.*, **108**, 3664 (1986).
[9] J. Papaioannou, N. Papadimitropoulos, I. Mavridis. *Mol. Phys.*, **97**, 611 (1999).
[10] G. Nolze, W. Kraus. *Powder Diffr.*, **13**, 256 (1998).
[11] N. Agmon. *Chem. Phys. Let.*, **244**, 456 (1995).
[12] B.V. Merinov. *Solid State Ionics*, **84**, 89 (1996).
[13] A. Oza. *Cryst. Res. Technol.*, **19**, 697 (1984).
[14] J. Papaioannou, V. Charalampopoulos, P. Xynogalas, K. Viras (to be published).
[15] L. Kloo, J. Rosdahl, P. Svensson. *Eur. J. Inorg. Chem.*, 1203 (2002).
[16] F. Demartin, P. Deplano, F.A. Devillanova, F. Isaia, V. Lippolis, G. Verani. *Inorg. Chem.*, **32**, 3694 (1993).
[17] A. Anderson, T.S. Sun. *Chem. Phys. Lett.*, **6**, 611 (1970).
[18] P. Svensson, L. Kloo. *J. chem. Soc. Dalton Trans.,* 2449 (2000).